Lipid-Induced Conformational Switch in the Membrane Binding Domain of CTP:Phosphocholine Cytidylyltransferase: A Circular Dichroism Study†

Svetla Taneva,‡ Joanne E. Johnson,‡ and Rosemary B. Cornell*,‡,§

Department of Molecular Biology and Biochemistry and Department of Chemistry, Simon Fraser University, Burnaby, British Columbia, Canada, V5A 1S6

Received July 14, 2003; Revised Manuscript Received August 11, 2003

ABSTRACT: CTP:phosphocholine cytidylyltranferase (CCT) regulates phosphatidylcholine (PC) biosynthesis. Its activity is controlled by reversible interactions with membrane lipids, mediated by an internal segment referred to as domain M. Although domain M peptides adopt an amphipathic α-helical structure when membrane bound, the structure of this domain in the context of the whole enzyme in the lipid-free and lipid-bound state is unknown. Here we derive lipid-induced secondary structural changes in CCTα using circular dichroism and three deconvolution programs. The analysis of two fragments, CCT236 (CCT1−236, housing the catalytic domain) and a synthetic domain M peptide (CCT237−293) aided the assignment of structural change to specific domains. To carry out this study, we developed a micellar lipid activating system that would avoid generation of CCT-induced lipid vesicle aggregates that interfere with the CD analysis. Lysophosphatidylcholine/phosphatidylglycerol (LPC/PG) mixed micelles supported full activation of CCT and caused an increase in the α-helix content of full-length CCT from 25 to 41%, at the expense of all other conformations. LPC/PG also induced an increase in α-helix content of the domain M peptide from 7 to 85% at the expense of all other conformers. This lipid system did not significantly affect the secondary structure of CCT236, nor did it affect the proteolytic fragmentation pattern of this region within full-length CCT, suggesting that the region containing the catalytic domain changes very little upon membrane activation of CCT. Our data suggest that lipids trigger a conformational switch in domain M from a mixed structure to an α-helix, thus creating a hydrophobic face for membrane insertion. Our results negate the idea that domain M is entirely helical in both the soluble and membrane-bound forms of CCT.

CTP:phosphocholine cytidylyltransferase (CCT)[1] catalyzes a rate-limiting and regulatory step in the synthesis of phosphatidylcholine (PC), a major component of eukaryotic cell membranes (*1*, *2*). CCT exists in both soluble and membrane-associated forms. The soluble form is inactive, whereas translocation of CCT to lipid membranes activates the enzyme. Membrane binding and activation of CCT are regulated by changes in membrane lipid composition and the phosphorylation state of CCT (*3*−*7*). In vitro, CCT binds to and is activated by lipid vesicles containing either anionic lipids or neutral lipids, which promote formation of nonbilayer phases (*8*−*10*). The binding is weak and reversible and involves both electrostatic and hydrophobic interactions (*7*, *9*, *11*, *12*).

Limited proteolysis (*13*) and functional analysis of mammalian CCT fragments (*14*−*17*) have revealed that it is organized into three discrete structural and functional domains. The domain structure of CCTα is diagrammed in Figure 1. A relatively compact N-terminal head (amino acids 1−236) contains the conserved catalytic domain between residues 75−236 (domain C). Residues 75−212 share 31% identity and ∼55% similarity with a bacterial glycerolphosphate cytidylyltransferase (GCT), whose structure has been solved (*18*). The fold of the catalytic domain, based on the GCT structure, conforms to a mononucleotide fold, characterized by alternating β-strands and helices linked by turns to generate a five-stranded parallel β-sheet flanked by helices. The secondary structure content of GCT obtained from its crystal structure is 36% α-helix, 25% β-strand, 34% turn + other. There is also a 3−10 helix segment (5%). No information on the structure of the N-terminal 75 amino acids of CCT (domain N) is available. The structure of the membrane-binding domain M (residues ∼237−299) in complex with SDS has been solved by two-dimensional NMR methods (*19*). It consists of a continuous α-helix for at least 50 residues linked via a turn to a loose coil at the N-terminus. The domain M helix has strong amphipathic properties (*20*, *21*). The C-terminal serine-proline rich region (domain P) is highly phosphorylated in vivo (*14*, *22*). Domain P is the most proteolytically sensitive region in both the

† This work was supported by the Canadian Institutes for Health Research, Grant MT-12134.

* To whom the correspondence should be addressed. E-mail: cornell@sfu.ca. Phone: 604−291−3709. FAX: 604−291−5583.

‡ Department of Molecular Biology and Biochemistry.

§ Department of Chemistry.

[1] Abbreviations: CCT, CTP:phosphocholine cytidylyltransferase; CD, circular dichroism; CMC, critical micelle concentration; DTT, dithiothreitol; GCT, CTP:glycerolphosphate cytidylyltransferase; LPC, 1-oleoyl-2-hydroxy-*sn*-glycero-3-phosphocholine; PC, phosphatidylcholine; PG, phosphatidylglycerol; OA, oleic acid; OG, *n*-octyl-β-D-glucopyranoside; PMSF, phenylmethylsulphonylfluoride; SUV, sonicated unilamellar lipid vesicles; SDS, sodium dodecyl sulphate.

10.1021/bi035234k CCC: $25.00
Published on Web 09/12/2003

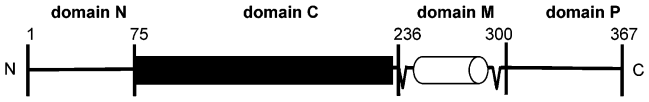

FIGURE 1: Domain structure of CCTα.

soluble and membrane-bound forms (*13*). Secondary structure algorithms indicate a lack of ordered structure for domain P.

Much evidence supports the concept that binding and intercalation of domain M into lipid membranes are responsible for lipid activation in vivo and in vitro (*13*, *15*−*17*). A catalytic fragment of CCT lacking domains M and P (CCT236) cannot be translocated to membranes and is constitutively active (*15*, *23*). These observations have led to a model of activation of CCT in which domain M is an inhibitor of the catalytic domain. Membrane binding of domain M relieves the inhibition and activates the enzyme (*2*, *15*, *23*).

CD measurements on synthetic peptides corresponding to domain M show that membrane binding is accompanied by a transition from random coil to α-helix (*20*, *21*). The membrane translocation of the peptide involves electrostatic localization on the membrane surface and intercalation of the amphipathic helix into the polar headgroup and interfacial region of the lipid bilayer (*12*, *20*, *21*). It is conceivable, however, given the strong predicted preference of the domain M sequence for an α-helical conformation, that domain M is helical in both the soluble and membrane-bound forms of the enzyme. Binding to membranes could involve a simple dislocation of the helix from contacts with the catalytic domain, where its interactions may inhibit catalysis. The results of the present study argue against this idea, and suggest instead that domain M is a mix of β-strand, turn, and unordered conformations in CCT's soluble form, and is transformed into an α-helix in the presence of a suitable helix-stabilizing membrane interface.

MATERIALS AND METHODS

Materials. Egg yolk phosphatidylcholine and phosphatidylglycerol were purchased from Northern Lipids Inc. 1-Oleoyl-2-hydroxy-*sn*-glycero-3-phosphocholine was from Avanti Polar Lipids, and oleic acid and *n*-octyl-β-D-glucopyranoside were from Sigma. The purity of phospholipid stocks was confirmed by thin-layer chromatography using chloroform/methanol/ammonia (65:35:5 v/v/v), and the concentrations were confirmed by phosphorus assay (*24*). CTP, dithiothreitol, phenylmethylsulfonylfluoride, DEAE-Sepharose, CM-Sepharose, Blue Sepharose (fast flow), ovalbumin (from chicken egg), and α-chymotrypsin were from Sigma.

Methods. Protein Expression and Purification. Rat liver CCTα isoform and CCTα236 (encoding amino acids 1−236) were expressed by baculovirus infection of *Trichoplusia ni* cells. The full-length wild-type CCTα was transferred from pAX142 (*25*) into the viral transfer vector pVL1393 (Pharmingen) at the *BamH*I/*Not*I sites. CCTα236 was engineered by PCR with a stop codon immediately following codon 236, a *Sal*I site immediately following the stop codon, and a *Bgl*II site before the start codon. The fragment excised with *Sal*I and *Bgl*II was filled in with DNA polymerase I and inserted into the *BamH*I/*Xba*I sites of pVL1393. Recombinant virus was created by cotransfection of *T. ni* cells with the resulting plasmid and BaculoGOLD AcNPV DNA (Pharmingen). Recombinant virus was subjected to three rounds of amplification as described in the product manual (Pharmingen) to produce high titer virus for infection of the *T. ni* cells. Cytosol was prepared as described (*26*) 2 days after infection. Full-length CCT was purified as described (*23*) with modifications (*10*). CCT236 was purified as described (*23*) with the following modifications: Cytosol containing CCT236 was diluted 5-fold in buffer A (10 mM Tris, pH 7.4, 1 mM EDTA, 2 mM DTT, containing a battery of protease inhibitors (*26*)), and the pH was adjusted to 6.0 prior to loading on the CM-Sepharose column which had been equilibrated in buffer A, pH 6.8. The slightly acidic pH improved retention of CCT236 on the resin. After 10 column volumes of buffer A, pH 6.8, CCT236 was eluted with buffer A, pH 7.5 containing 0.15 M NaCl. The CM-Sepharose activity pool was loaded onto a Blue-Sepharose column equilibrated with buffer A containing 0.15 M NaCl. The column was washed with 10 column volumes of buffer A containing 0.2 M NaCl and CCT236 was eluted with buffer A containing 0.6−0.75 M NaCl. The pure enzymes were stored in aliquots at −80 °C and their concentrations were determined by quantitative amino acid analysis (Alberta Peptide Institute, Edmonton, Alberta). The purity of the two CCTs is shown in Figure 8, lanes 1 and 2. The contaminant in the CCT236 sample at ∼24 kDa was only observed with silver stain. This band was not observed with Coomassie Blue staining of 10 times the sample mass.

Peptide Synthesis. A 57-mer peptide corresponding to residues 237−293 of rat liver CCTα was synthesized on an ABI model 431A peptide synthesizer using Fmoc chemistry by Dr. Krystyna Piotrowska at the University of British Columbia Peptide Service Laboratory (Vancouver, BC). The peptide was acetylated at the N-terminus and aminated at the C-terminus to eliminate the influence of the charged terminal groups. It was HPLC purified to >99% purity and MALDI-TOF revealed its mass to be 7073.8 Da (theoretical = 7072.3). The concentration of an aqueous stock solution (1 mM) was determined by measuring the absorbance at 280 nm (ϵ_{280} = 6970 M^{-1} cm^{-1}).

Preparation of Small Unilamellar Vesicles (SUVs) and Mixed Micelles, and Vesicle Aggregation Assay. Phospholipid stocks were made in chloroform (PC, LPC) or chloroform/methanol (3:1, vol/vol) (PG). Their concentrations were determined by phosphorus assay (*24*). SUVs were prepared by mixing lipids in chloroform, evaporating the solvent, resuspending in buffer, and sonicating as described previously (*27*) except the buffer was 50 mM phosphate, pH 7.0. Micellar solutions of LPC and LPC/PG were prepared at different molar ratios using the same procedure. Aggregation of phospholipid SUVs and mixed micelles induced by CCT was assayed at 20 °C by measuring the increase in sample turbidity after addition of the protein using a Beckman DU600 spectrophotometer. The vesicles (0.25 mM) or mixed micelles (1 mM) were added to a quartz cell, stirred, and the absorbance at 400 nm recorded. After 3 min, CCT was added to the sample cell to a final concentration of 0.3 μM, the sample was mixed by rapid pipetting, and the absorbance was recorded for 5 min. The contribution of 0.3 μM CCT to the solution turbidity in the absence of lipid was negligible.

CCT Activity Assay and Chymotrypsin Digestion. CCT activity was determined essentially as described (*28*). Partial proteolysis using α-chymotrypsin was performed as described (*13*) using 2−2.5 μM full-length CCT and 4 μM CCT236 in a 30 μL reaction volume. The CCT/chymotrypsin weight ratio was 150:1. At different times aliquots of the reaction mixture were removed and the digestion was stopped with PMSF, final concentration of 2 mM. The fragments were separated by SDS−PAGE using 12 or 13% acrylamide, and were visualized with silver (*29*) or Western blotting as described (*30*) with an antibody directed against the N-terminal 15 amino acids (*14*) or domain M (*17*).

Circular Dichroism and Deconvolution. CD measurements were acquired for full-length CCT, CCT236, and domain M peptide in solution and in mixtures with sonicated lipid vesicles or micelles. Samples were prepared in 50 mM phosphate buffer (pH 7.0). CD spectra were recorded using a Jasco-J-710 spectropolarimeter at 20 °C in a cell of 1-mm path length at a scanning rate of 50 nm/min, a time constant of 0.25 s, and a bandwidth of 1 nm. Spectral resolution was 0.5 nm, and 20 scans were averaged per spectrum. All spectra were smoothed and corrected for the appropriate backgrounds: buffer or buffer + lipid at corresponding concentrations for the lipid−protein samples. Molar ellipticity was expressed as deg cm^2/dmol based on molecular masses of 41 700 Da and 367 amino acids for full-length CCT, 26 750 Da and 236 amino acids for CCT236 (*23*), and 7072 Da and 57 amino acids for the domain M peptide. The content of secondary structure was deconvoluted from the CD spectra by three methods, SELCON 3, CONTINLL, and CDSSTR, which are part of the software package CDPro available at http://lamar.colostate.edu/∼sreeram/CDPro (*31*). The strengths and limitations of the three deconvolution programs we selected have been reviewed (*31*−*34*)**.** The three programs used an identical set of 23 reference proteins selected by the program CLUSTER included in the software package. CLUSTER determines the tertiary class and creates a tertiary class-specific subset of reference proteins (*35*). The three methods have similar overall performance indices (RMS deviation between the X-ray and CD-predicted values of secondary structure = 6.8%). Analyzing protein CD spectra using all three methods improves the reliability of the predicted secondary structure (*31*). In addition, the CD spectra of ovalbumin in 50 mM phosphate buffer (pH 7.0) acquired on our instrument and analyzed with the three programs in CDPro revealed 28% helical structure, 21% β, 22% turn, and 29% unordered conformations. This is reasonably consistent with the values obtained from the X-ray structure of ovalbumin of 31% α-helix, 28% β, 17% turn, and 24% unordered (*36*). Ovalbumin was selected as a test protein because it has secondary structure content similar to CCT.

CCT Secondary Structure Prediction. The secondary structure of full-length CCT (CCT367), CCT236, and the domain M peptide were predicted by PsiPred (*37*) and PROFsec (*38*). The methods have average accuracies for the expected three states (helix, strand, and coil) of nearly 78% for PsiPred and 76% for PROFsec. They correctly identified within the catalytic domain of CCT 5/5 α-helices, the 3/10 helix segment and 4/5 (PsiPred) and 5/5 (PROFsec) β-strands that have been observed in the X-ray structure of GCT (*18*).

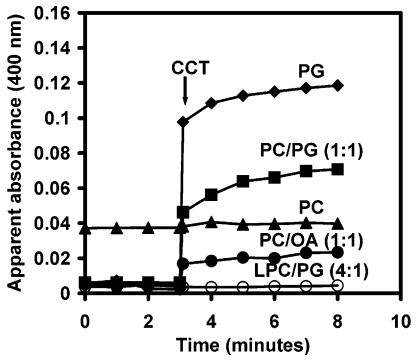

FIGURE 2: CCT-induced aggregation of SUVs. The lipid ratios are molar. Lipid concentrations were 0.25 mM (SUVs) and 1 mM (micelles). The CCT concentration was 0.3 μM. The arrow indicates the time of CCT addition.

RESULTS

Development of an Activating Micellar Lipid System Suitable for CD Analysis. SUVs composed of anionic phospholipids such as PG are commonly used CCT-lipid activating systems. Our initial CD spectra of full-length CCT plus SUVs of PG and PC/PG (1:1, mol/mol) showed significant flattening in the 205−225 nm region compared to spectra of lipid-free CCT. The degree of sample noise below 200 nm was also amplified, leading to loss of signal intensity in this region. Because light scattering due to large vesicles or aggregated vesicles could generate such effects (*39*, *40*), we performed separate experiments to assess the aggregation of lipid vesicles by CCT, by monitoring sample turbidity as a function of time after addition of CCT (Figure 2). The CCT-dependent increase in the apparent absorbance at 400 nm was dependent on the lipid composition and correlated with the degree of vesicle negative charge (Figure 2). Thus, no aggregation was observed when the vesicles were composed of PC, which does not promote CCT binding (*7*, *8*), and the greatest degree of aggregation was observed with 100% PG, the vesicle with highest affinity for CCT (*7*, *8*).

To overcome the negative turbidity effects of CCT-induced aggregation of SUVs on CD measurements, we explored mixed micelle systems. Triton X-100 mixed micelles containing acidic lipid are known to activate CCT (*27*), but Triton's strong absorption in the wavelength range used for CD precluded its use. We monitored the optical densities of mixtures of LPC containing negatively charged PG to determine the bilayer to micelle transition (*41*, *42*). We found that at concentrations of LPC above the CMC (0.02−0.2 mM) (*43*) and above a 1/1 molar ratio of LPC/PG, sample turbidity (A_{400}) was the same as that of LPC alone (data not shown). The turbidity of a mixture of LPC/PG (4:1, mol/mol) was very low and was not affected by the addition of CCT (Figure 2), indicating its potential suitability as a membrane mimic for the CD measurements.

Comparison of Micelles vs Vesicles as CCT Activators. We compared the activation of CCT by mixed micelles of LPC/PG (4:1, mol/mol) to the activation by SUVs composed of PG or PC/OA (Figure 3). The three systems containing negatively charged lipids activated CCT similarly (10−20-fold) over a broad range of concentrations (5−1000 μM). The LPC/PG micelles are therefore good mimics of membrane systems with respect to CCT activation. Pure lysoPG

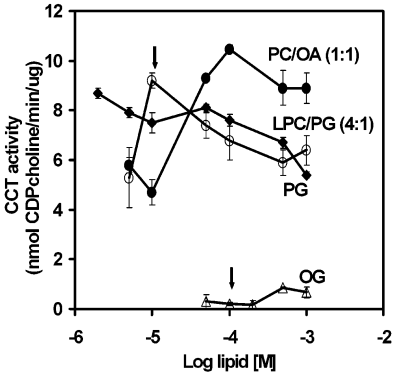

FIGURE 3: Dependence of CCT activity on the concentration of various lipid systems. The lipid ratios are molar. The concentration of CCT in the assay was 20 nM. Black arrows indicate CCT/lipid ratios of 500:1 (LPC/PG and PC/OA) and 5000:1 (OG). These are identical to those used in the CD measurements. The data for OG and LPC/PG represent the average of two experiments ± half range. The data for PG and PC/OA represent duplicates of a single experiment. In the absence of lipid the CCT specific activity is 0.5 nmol min^{-1} μg^{-1}.

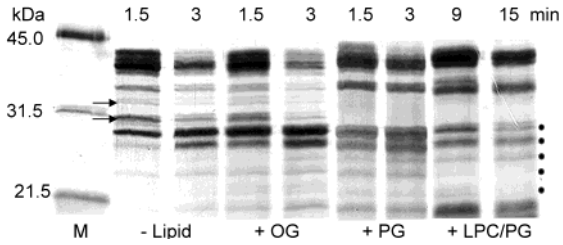

FIGURE 4: Comparison of the chymotrypsin digestion pattern of CCT in the absence and presence of lipid. The concentration of CCT was 2 μM. The lipid concentrations were 10 mM (OG), 0.8 mM (PG), and 0.8 mM (LPC/PG). Aliquots were removed at the indicated time points and quenched with 2 mM PMSF. M = standard molecular mass markers. Arrows indicate the positions corresponding to 30 and 33 kDa doublets. N-terminal fragments are indicated by ●.

micelles were tested as a membrane mimic, but did not activate at concentrations above the CMC (0.16 mM; *44*). Figure 3 also shows that the nonionic detergent OG did not activate CCT at the concentrations measured.

To test that CCT interacts in a similar manner with LPC/PG micelles and anionic vesicles, we compared the ability of the lipid systems to protect sites in domain M from proteolytic cleavage. The products of partial proteolysis of CCT by chymotrypsin have been previously characterized (*13*, *14*, *17*). Digestion proceeds progressively from the more loosely structured C-terminal tail (composed of domains M and P). Following cleavage of the tail, digestion of the more compact core of domains N + C proceeds from its C-terminus (*13*). Chymotrypsin digestion revealed several differences in the cleavage patterns of soluble compared to membrane-bound CCT. With the lipid-free form there were two sets of fragments running as ~33 and ~30 kDa doublets (Figure 4, arrows). These fragments were also produced by chymotrypsin digestion of CCT in the presence of the nonactivating detergent, OG (Figure 4). By contrast, the 30- and 33-kDa cleavage fragments were not detected at any time point in the proteolytic digestion of CCT in the presence of the activating lipids PG or LPC/PG (Figure 4). The identity of three of the bands that are missing from the digests done in the presence of activating lipids has been determined using

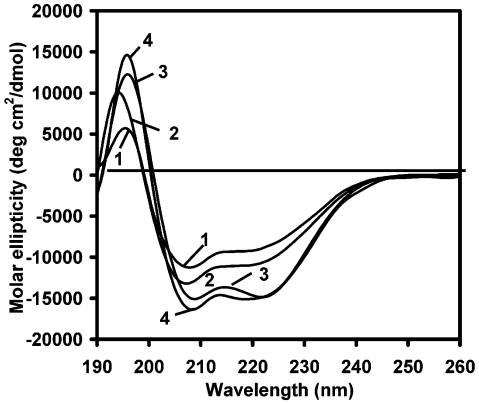

FIGURE 5: CD spectra of full-length CCT: 50 mM phosphate buffer (1), 10 mM OG (2), 0.8 mM PC/OA (1:1, mol/mol) (3), and 1 mM LPC/PG (4:1, mol/mol) (4). The concentration of CCT was 2 μM. The spectra are averages of two independent determinations.

mass spectrometry: 1−234; 1−240; and 1−263 (M. Bogan, G. Agnes, and R. B. Cornell, unpublished observations). A complete presentation of the proteolysis pattern and fragment identification of soluble and micelle-bound CCT will be presented elsewhere. Thus, there are at least three cleavage sites in domain M that are protected from proteolysis in the membrane or micelle-bound form of CCT. This suggests that domain M is buried in both the micelle and vesicle bound forms of CCT.

One difference that was noted between the micelle and vesicle system is that the rate of digestion was slower in the presence of the micelles (Figure 4, note the different digestion times). This slower digestion is not due to inhibition of chymotrypsin by the micelles, since the rate of hydrolysis of the substrate, *N*-benzoyl-L-tyrosine ethyl ester, was identical in the presence and absence of 1 mM LPC/PG (4/1). It appears that LPC/PG micelles bind the CCT C-terminus in a manner that decreases the accessibility of cleavage sites in this domain. However, the pattern of bands in the 22−27 kDa range was the same as in PG vesicle-bound samples. These fragments contain the N-terminus of CCT but not domain M, based on antibody reactivity (Figure 8). Thus, for LPC/PG-bound CCT, once the C-terminal domain of CCT is cleaved the fragmentation of the catalytic domain is the same as for CCT bound to PG vesicles, indicating a similar conformation in either lipid system. The same fragmentation of the catalytic domain was also observed in lipid-free CCT (Figure 4; fragments indicated by solid circles), indicating that lipids have little effect on the conformation of this domain.

CD Analysis of Full-Length CCT Indicates a Lipid-Triggered Increase in α-Helix Structure. The CD spectra of CCT were measured in the presence and absence of three lipid systems (Figure 5). OG was used as a reference nonactivating amphiphile, while LPC/PG (4/1) and PC/OA (1/1) were used as lipid activators (see Figure 3). High lipid/CCT ratios were used (400−500) to ensure complete protein binding and to prevent potential artifacts due to CCT-induced aggregation in the lipid systems.

The CD spectrum of CCT in phosphate buffer displayed a positive maximum at ~195 nm and double minima at ~208 and ~222 nm, indicative of some α-helical character (*45*). The addition of OG, PC/OA, or LPC/PG caused an increase in the intensity of these maximum and minimum ellipticities,

Table 1: Secondary Structure of Full-Length CCT[a]

	Program	Buffer	OG 10mM	LPC/PG 1mM	PC/OA 0.8mM
%Helix	SELCON3	24 ± 0.4	27.9 ± 0.1	36.0 ± 5.0	31.5 ± 0.1
	CONTINLL	22 ± 4.0			
	CDSSTR	29 ± 6.0	38.4 ± 0.6	46.0 ± 1.0	46.7 ± 0.9
	Average	25.0	33.0	41.0	39.0
%β-Strand	SELCON3	24.6 ± 0.2	17.8 ± 0.7	13.0 ± 6.0	17.0 ± 3.0
	CONTINLL	21.5 ± 1.0			
	CDSSTR	18.2 ± 4.1	13.6 ± 1.2	21.0 ± 1.5	19.0 ± 1.0
	Average	21.4	15.7	17.0	18.0
% Turn	SELCON3	26.0 ± 3.0	26.8 ± 0.4	27.0 ± 5.0	25.0 ± 3.0
	CONTINLL	30.0 ± 4.0			
	CDSSTR	29.3 ± 0.2	29.3 ± 0.6	17.0 ± 2.0	18.7 ± 0.6
	Average	28.4	27.6	22.0	22.0
% Unordered	SELCON3	26.4 ± 1.2	26.9 ± 0.4	25.5 ± 3.0	28.0 ± 1.0
	CONTINLL	26.0 ± 1.0			
	CDSSTR	22.0 ± 3.0	19.1 ± 1.4	15.0 ± 1.0	16.0 ± 2.0
	Average	25.0	23.0	20.0	22.0

[a] The spectra in Figure 5 were deconvoluted using the three programs in CDPro suite. Using CONTINLL, the reproducibility of the deconvolution of two independently obtained spectra of CCT in the presence of OG, LPC/PG, or PC/OA was poor. Thus, we did not include the data.

indicative of higher helical content. OG had the least pronounced effect on the ellipticity of CCT. The negative portion of the spectra of CCT in the presence of LPC/PG or PC/OA was nearly superimposed, whereas there was a difference in the intensities at ~195 nm. Stronger light scattering at the short wavelengths in the PC/OA system may account for the decrease in the ellipticity, since CCT induced some aggregation in PC/OA, but not LPC/PG (Figure 2).

The CD spectra in Figure 5 were deconvoluted using SELCON 3, CONTINLL, and CDSSTR to obtain the secondary structure distribution of CCT (Table 1). In buffer alone, CCT exhibits approximately equal contents of helix, strand, turn, and unordered conformations. This distribution is fairly consistent among the three programs. In the presence of OG, there was a small increase in α-helix at the expense of *β*-strand. These changes were within the accuracy of the SELCON3 method (RMSD ≅ 5%; *31*) and were significant only for α helix content based on CDSSTR. In contrast, LPC/PG induced a significant change in the secondary structure of CCT (Table 1). Both SELCON3 and CDSSTR indicated an increase in the helical content of 12 and 17%, respectively. Using CONTINLL, the reproducibility of the deconvolution of two independently obtained spectra of CCT in the presence of lipids was poor; the deviations were greater than expected based on the performance indices published for this program (*31*); thus, we did not include the CONTINLL results in our averaging. On the basis of the averages of SELCON3 and CDSSTR, the increase in helix content was accompanied by small losses in *β*-strand, turn, and unordered structure. Deconvolution of the CD spectra of CCT in the presence of PC/OA also showed an average increase in the helical content to about 39% at the expense of all other conformers. The light scattering interference with PC/OA (Figure 2) may have compromised accuracy somewhat; however, the same trends are observed for both lipid systems. Thus, it appears that membrane translocation of CCT was accompanied by a conformational change that increased its helix content by ~58 amino acids and decreased the content of *β*-strand, turns, and unordered conformers by ~17, 23, and 18 amino acids, respectively (Table 4).

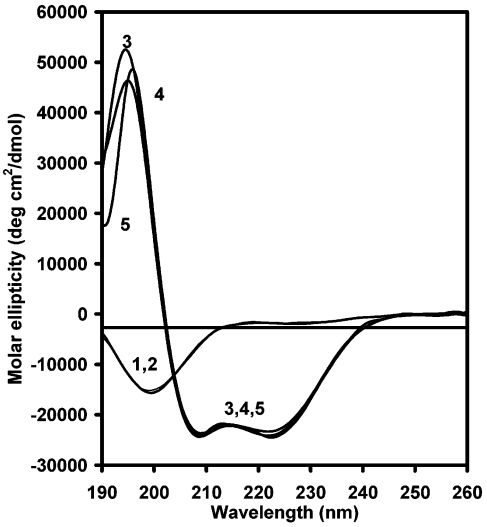

FIGURE 6: CD spectra of domain M peptide: 50 mM phosphate buffer (1), 10 mM OG (2), 1 mM LPC/PG (4:1, mol/mol) (3), 0.8 mM PC/OA (1:1, mol/mol) (4), and 0.8 mM PG (5). The concentration of domain M peptide was 12 *μ*M.

CD Analysis of the Domain M Peptide Reveals Strong Helix Stabilization by Lipid Micelles and Vesicles. The CD spectra of domain M peptide in buffer or in the presence of OG were typical for predominantly random coil conformation as seen by the single negative maximum at 200 nm (Figure 6). However, in the presence of LPC/PG micelles, or vesicles of PC/OA or PG, the CD spectra were characteristic of α-helices (strong positive band at ~195 nm; strong minima at ~208 and ~222 nm). It is noteworthy that this peptide, unlike full-length CCT, did not induce aggregation of anionic SUVs (data not shown). Therefore, the CD spectra of the peptide in the presence of SUVs were not affected by turbidity contributions from aggregates and were identical to the spectra taken in the presence of micelles of LPC/PG.

The secondary structure of the domain M peptide was deconvoluted from the CD spectra using all three programs, and the results were consistent among the three (Table 2). In buffer the peptide had about 7% α-helix, ~30% *β*-strand, ~60% turn + unordered conformations. This distribution was not changed by OG. The three activating lipid systems increased the α-helix content to a similar level of about 80% at the expense of *β*-strand, turn, and unordered, and nearly eliminated the *β* character from the spectra.

CD Analysis of CCT236 Reveals Very Little Effect of Lipids on Secondary Structure. The spectrum for CCT236 in buffer displayed negative minima at ~208 and ~222 nm (Figure 7). Unlike full-length CCT, the addition of CCT236 to anionic vesicles such as PG did not induce aggregation (data not shown). To be consistent with the CD analyses performed on full-length CCT, we analyzed the effect of LPC/PG micelles on CCT236. LPC/PG induced a very small change in the molar ellipticity. Deconvolution of these spectra using all three programs indicated a distribution of about 38% α-helix, 16% *β*-strand, 18% turn, and 29% unordered (Table 3). None of the deconvolution methods indicated significant change in the fractions of secondary

Table 2: Secondary Structure of Domain M Peptide[a]

	Program	Buffer	OG 10mM	LPC/PG 1mM	PC/OA 0.8mM	PG 0.8mM
%Helix	SELCON3	10	14.8	78	73.1	74.4
	CONTINLL	7.9	8.2	95	76.1	77.1
	CDSSTR	4.2	4.1	82.5	73.4	87.5
	Average	7.4	9.0	85.1	74.2	79.7
%β-Strand	SELCON3	29.8	31.5	-2.0[b]	-1.7[b]	-1.3[b]
	CONTINLL	30.0	29.5	5.1	0.4	0.3
	CDSSTR	33.0	33.3	5.2	8.5	1.8
	Average	30.9	31.4	2.8	2.4	0.3
% Turn	SELCON3	22.2	22.1	12	9.4	9.5
	CONTINLL	23.5	23.5	0	5.4	9.8
	CDSSTR	23.2	22.9	6.9	7.8	5.9
	Average	23	22.8	6.3	7.5	8.4
% Unordered	SELCON3	34.4	32	12.9	19.7	18
	CONTINLL	38.7	38.8	0	18.1	12.8
	CDSSTR	38.4	38.3	4.4	9.6	3.7
	Average	37.2	36.4	5.8	15.8	11.5

[a] The spectra in Figure 6 were deconvoluted using the three programs in CDPro suite. [b] SELCON3 (and CDSSTR) allow small negative percentages that are within experimental error.

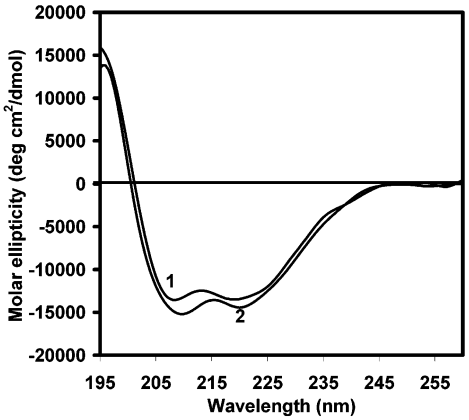

FIGURE 7: CD spectra of CCT236: 50 mM phosphate buffer (1) and 0.5 mM LPC/PG (4:1, mol/mol) (2). The concentration of CCT236 was 2 μM. The spectra are representative of two independent experiments.

structure for CCT236 in the presence of LPC/PG (Table 3). In separate measurements, we tested the influence of lipids on the activity of CCT236. It was active independently of the presence of 0.2 mM SUVs of PC/OA vesicles or a range of LPC/PG (4/1) micelle concentrations from 5 μM to 1 mM (5.7 nmol min^{-1} μg^{-1} in the absence of lipid, and 5.5 nmol min^{-1} μg^{-1} in the presence of 0.5 mM LPC/PG). Thus, in agreement with Friesen and Kent (*23*), this truncated form of CCT is constitutively active.

It is conceivable that the secondary and tertiary structure of the CCT1−236 fragment differs from that of amino acids 1−236 within full-length CCT. To explore this possibility, we compared the chymotrypsin digestion pattern of the two CCTs (Figure 8). Digestion of both proteins generated a set of five fragments with apparent M_r between 22 and 27 kDa that react with antibody against the CCT N-terminus, but not with antibody against domain M. This analysis indicates that the accessibility of these sites of cleavage within domain C is identical in truncated and full-length CCT. Thus,

Table 3: Secondary Structure of CCT236[a]

	Program	Buffer	LPC/PG 0.5mM
%Helix	SELCON3	36.6	33.8
	CONTINLL	34.8	33.9
	CDSSTR	43.6	47.1
	Average	38.3	38.3
%β-Strand	SELCON3	17.8	15.4
	CONTINLL	16.4	14.2
	CDSSTR	15.6	15.0
	Average	16.6	14.9
% Turn	SELCON3	20.5	22.5
	CONTINLL	20.3	25.9
	CDSSTR	11.9	12.3
	Average	17.6	20.2
% Unordered	SELCON3	28.4	28.6
	CONTINLL	28.4	29.4
	CDSSTR	29.7	26.7
	Average	28.8	28.2

[a] The spectra in Figure 7 were deconvoluted using the three programs in CDPro suite.

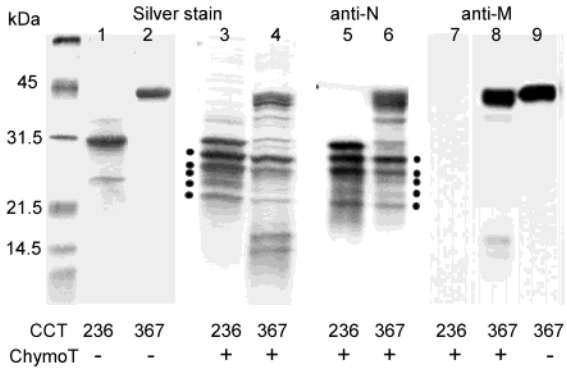

FIGURE 8: Proteolytic fragmentation of full-length CCT (CCT367) and CCT236. The samples were digested with chymotrypsin (ChymoT) for 2.5 min. Lanes 1−4, silver stain; lanes 5 and 6, Western blot with antibody against the N-terminal 15 residues; lanes 7−9, Western blot with antibody against domain M (residues 256−288). The N-terminal fragments of CCT236 that are also observed upon digestion of CCT367 are indicated by ●.

CCT236 is a very good mimic of domains N + C within full-length CCT.

DISCUSSION

LPC/PG Micelle System Mimics Membrane Activators and Is Suitable for CD Measurements. SUVs can be used for CD analysis if they are monodisperse and of sufficiently small diameter to display minimal scattering (*39*). In our trials with CCT, we found that anionic phospholipid vesicles, which are commonly used as CCT activators, were aggregated by the addition of CCT. This caused a degree of light scattering that compromised their use for deconvolution of secondary structure from the spectra. The induction of anionic vesicle aggregation by full-length CCT (but not by domain M peptide or by CCT236) is interesting and will be the subject of a separate paper.

Light scattering artifacts were eliminated by use of mixed micelles of LPC/PG (4:1, mol/mol). Micelles of lysophos-

Table 4: Estimated Number of Amino Acids in Each Secondary Structural Element of CCT Domains[a]

domain	residues	LPC/PG	α-helix	β-strand	turn	unordered
full	1−367	−	92	79	104	91
		+	150	62	81	74
N + C	1−236	−	90	39	42	68
		+	90	35	47	66
M	237−293	−	4	18	13	21
		+	49	2	4	3

[a] The number of amino acids representing each secondary structure element is reported based on the average percentage values reported in Tables 1−3. The deconvolution programs allow the sum of the percent secondary structures to be 100 ± 5%, which explains why the amino acid totals in CCT or a domain of CCT may be within 5% of the actual number of amino acids.

pholipids are generally smaller than 10 nm in diameter, they do not exhibit substantial scattering, and they have been extensively used in CD measurements as mimics for the phospholipid environment for proteins (*46*−*51*). The dispersion state of micelles of LPC/PG (4:1, mol/mol) was not affected by CCT (Figure 2). Of the vesicle systems, CCT induced the least aggregation of PC/OA (1/1) SUVs. This was the only lipid vesicle system amenable to CD analysis. The LPC/PG micelles and PC/OA vesicles fully activated CCT (Figure 3). Moreover, burial of domain M was implicated in both the micelle and vesicle systems, as assessed by protection from proteolysis (Figure 4). Both micelle-bound and vesicle-bound CCT generated the same fragmentation pattern for domains N + C, suggesting that these domains have the same tertiary fold when bound to either lipid system (Figure 4). Finally, the CD changes obtained with the micelle system were mimicked by PC/OA vesicles.

Secondary Structure of Soluble and Lipid-Activated CCT Calculated from CD. Previously, CD analysis of domain M peptides suggested that activating lipid vesicles promote a conversion from unordered to α-helical secondary structure (*12*, *20*, *21*). The spectra in those studies were not deconvoluted; the helical content was merely estimated from the ellipticity at 222 nm. To determine whether domain M undergoes a disordered to helix transition upon membrane binding in the context of the entire enzyme, we deconvoluted CD spectra of full-length CCT, a fragment comprising domains N + C (CCT236), and a 57mer domain M peptide, in the absence and presence of activating lipids. This allowed assignment of secondary structure elements to CCT's individual domains.

For full-length CCT in its soluble form, the three deconvolution methods generated a consensus structure of approximately equal parts of the four conformations. In the presence of activating lipids SELCON3 and CDSSTR indicated an increase of α-helix, but whereas SELCON3 showed the increase entirely at the expense of β-strand, CDSSTR indicated decreases in turn and unordered conformation. Thus, we conclude that upon dissociating from membranes the equivalent of ∼58 amino acids converts from an α-helical structure probably to a mixture of other conformations (Table 4). We are proposing that this conformational switch occurs in domain M.

The Lipid-Dependent Change in Secondary Structure Occurs Outside of Domains N + C. We found that the secondary structure of CCT236 was not significantly altered by the activating lipid micelles. However, this observation alone does not imply that domains N + C are unaltered when full-length CCT binds membranes, since CCT236 lacks a lipid binding domain. More revealing is our finding that the proteolytic sensitivity of domains N + C within full-length CCT is not affected by activating lipids (Figure 4). This implies that the lipid-dependent secondary structure change lies outside the N-terminal domains, and is associated with domain M or P. That lipids do not alter the fragmentation pattern of domains N + C leads to the important conclusion that only subtle changes in CCT's catalytic domain accompany the activation of the enzyme by the lipid interactions of domain M; changes that cannot be detected by chymotrypsin sensitivity.

The Lipid-Dependent Change in Secondary Structure Occurs in Domain M. We found that the helix content of full-length CCT in its soluble form could be accounted for by the helix content of CCT236 (∼90 residues as α-helix; Table 4). This suggests that the helix content of domain M and P in soluble CCT is very low. This statement stands only if CCT236 is an accurate conformational mimic of domains N + C within full-length CCT. Two observations suggest that this is true. First, CCT236 is a catalytically active form, suggesting that its fold would mimic that of domains N + C in lipid-bound CCT. Second, proteolysis of full-length CCT with chymotrypsin generates a set of fragments in the 27−22 kDa range, all of which bear the N-terminus. These same fragments are generated when CCT236 is digested (Figure 8). This suggests that the tertiary fold of the region between amino acids 1−236 within full-length CCT is the same as that of the CCT236 fragment.

The lipid-induced increase in helical content of full-length CCT (∼58 amino acids) can be roughly accounted for by the additional helical residues in domain M in its membrane-bound form. The helical content of domain M peptide increased from 4 to 49 amino acids upon addition of lipids (Table 4). There is a sound basis for accepting that the conformation of domain M within membrane-bound full-length CCT is also predominantly helical. Helix formation is promoted at amphipathic surfaces where peptide backbone hydrogen bonding is favored, and a low dielectric environment is presented for the favorable partitioning of the hydrophobic face of the helix (*52*). That domain M of CCT inserts into the bilayer upon binding has been established by lipid photolabeling (*17*), by protease protection (*13*; Figure 4 of this work), and by evaluation of the effects of lipid phase transitions on CCT binding (*8*, *11*). The energetic penalty for insertion of a single polypeptide strand with a non-hydrogen-bonded backbone precludes insertion as any conformation other than helix.

The secondary structure distribution of lipid-bound domain M and CCT236 as reported here are reliable estimates of the structure of these domains in full-length CCT. The CD-based secondary structure assignments for these domains as well as whole CCT *in the lipid-bound form* agree well with secondary structure prediction algorithms (Table 5). The predictions assign 77−88% helical content to the sequence corresponding to domain M. The conformation of domain P was not separately determined in our study, and it would probably be inaccurate to assign its structure by subtraction of the other domains from the full-length conformations. The predictive algorithms indicate a low content of structure

Table 5: Comparison of the Predicted Secondary Structures of CCT and CCT Domains and Those Determined from the CD Spectra of Full-Length CCT (CCT367), CCT236, and Domain M Peptide in the Presence of LPC/PG

	CCT367			CCT236			domain M peptide			domain P	
	PROFsec	PsiPred	CD	PROFsec	PsiPred	CD	PROFsec	PsiPred	CD	PROFsec	PsiPred
% helix	40	43	41	30	35	38	88	77	85	13	12
% β-strand	8	6	17	15	11	15	0	0	3	11	5
% Other	52	51	42	55	54	47	12	23	12	76	83

(Table 5). Only the region between amino acids 298−313, just preceding the phosphorylation sites, is predicted to have helix content. One possibility is that this region also converts from an unordered to an α-helix conformation upon lipid binding of CCT, thus accounting for the excess helical content of whole CCT (∼13 amino acids) that cannot be attributed to the region corresponding to the domain M peptide (Table 4). In fact, the membrane-binding domain may include this second inducible helix which we refer to as part of domain P in this paper.

Our CD data eliminate the model that domain M is helical in both soluble and membrane-bound forms of CCT. What then is the conformation of domain M in the soluble form of CCT? Unfortunately, the two deconvolution programs did not agree on whether the loss of helix upon desorbing from lipids generates a gain in β-strand, turn, or unordered. The conformation of domain M peptide in buffer is 7% helix, 31% strand, 23% turn, 37% unordered, but this peptide conformation may not closely mimic the conformation of domain M within the soluble form of full-length CCT. Since the predictive algorithms indicate a strong preference for the domain M sequence to adopt helical structure (Table 5), why then is it nonhelical in the soluble form of CCT? Domain M is very hydrophilic overall with 28 of its 57 residues bearing charges (ΔG values for transfer to water are negative, based on a variety of polarity scales; *53*). This explains why even unfolded conformers can accumulate in aqueous environments (*19*), and suggests why many conformations would be possible for the domain M segment in CCT's soluble form. There is not a sufficient energetic penalty associated with the exposure of the nonpolar side chains of domain M to force their burial from water. However, in the presence of an amphipathic membrane surface the formation of a helix lowers the free energy by peptide backbone hydrogen-bonding (freeing bound water to reduce ΔG by 0.4−0.5 kcal/mol per hydrogen bond; *52*) and by eliminating the hydrophobic penalty associated with exposure of the 22 nonpolar side chains. In theory, an amphipathic docking surface on CCT could also stabilize helix formation of domain M. Apparently none is available on domains N, C, or P of CCT.

Creation of α-Helical Domains as a Common Strategy for Membrane Binding. The lipid-triggered transition of the membrane binding domain of CCT from a mixture of strand, turn, and unordered conformers to an ordered continuous α-helix has precedence in the mechanisms of membrane interaction of a few other proteins. EPR analyses of spin-labeled apolipoprotein A1 (ApoA1) suggest a helix−loop−strand−helix structure in the lipid-free form (*54*). In the presence of lipids, the structure converts to a single continuous amphipathic α-helix that may form a belt around the lipidic HDL particle. The influenza hemagluttinin (HA-2) has an N-terminal hydrophobic peptide that functions as a membrane fusogen, but only at acidic pH. In the neutral pH conformation, the N-terminal region of HA-2 is a helix−loop−helix conformation that is postulated to be in a metastable state with the fusion peptide buried. Low pH-triggered transformation of the central coiled region into a helix generates an extended 66 residue helix that exposes the fusogenic hydrophobic peptide (*55*). Acidic phospholipids also trigger a disordered to amphipathic helix conformational switch in the membrane binding domains of the enzyme IIA component of the E. coli phosphotransferase system (*56*), and regulators of G protein signaling (e.g., RGS4; *57*). These conformational switches are, as in the case of CCT, important for the membrane interactions of these proteins and for their biological functions.

Since we have found that domain M is nonhelical in the soluble form of CCT, the next important objective will be to elucidate what that structure is, how it is maintained, and how acidic lipids transform it to an extensive amphipathic α-helix. The picture emerging for the conformational changes associated with lipid activation of CCT is one involving a large change in the structure of domain M, which confers only a subtle structural change in the catalytic domain to enhance the enzymatic efficiency by a factor of ∼100 (*23*). The nature of this subtle change at the active site presents a challenge for future research.

ACKNOWLEDGMENT

We thank Dr. Mark Paetzel for comments on the manuscript.

REFERENCES

1. Cornell, R. B. (1996) *Adv. Lipobiol. 1*, 1−38.
2. Kent, C. (1997) *Biochim. Biophys. Acta 1348*, 79−90.
3. Wang, Y., MacDonald, J. I. S., and Kent, C. (1993) *J. Biol. Chem. 268*, 5512−5518.
4. Houweling, M., Jamil, H., Hatch, G., and Vance, D. E. (1994) *J. Biol. Chem. 269*, 7544−7551.
5. Wang, Y., and Kent, C. (1995) *J. Biol. Chem. 270*, 17843−17849.
6. Yang, Y., and Jackowski, S. (1995) *J. Biol. Chem. 270*, 16503−16506.
7. Arnold, R. S., De Paoli-Roach, A., and Cornell, R. B. (1997) *Biochemistry 36*, 6149−6156.
8. Cornell, R. B. (1991) *Biochemistry 30*, 5881−5888.
9. Cornell, R. B. (1998) *Biochem. Soc. Trans. 26*, 539−544.
10. Davies, S. M. A., Epand, R. M., Kraayenhof, R., and Cornell, R. B. (2001) *Biochemistry 40*, 10522−10531.
11. Arnold, R. S., and Cornell, R. B. (1996) *Biochemistry 35*, 9917−9924.
12. Johnson, J. E., Xie, M., Sing, L. M., Edge, R., and Cornell, R. B. (2003) *J. Biol. Chem. 278*, 514−522.
13. Craig, L., Johnson, J. E., and Cornell, R. B. (1994) *J. Biol. Chem. 269*, 3311−3317.
14. Cornell, R. B., Kalmar, G. B., Kay, R. J., Johnson, M. A., Sanghera, J. S., and Pelech, S. P. (1995) *Biochem. J. 310*, 699−708.
15. Wang, Y., and Kent, C. (1995) *J. Biol. Chem. 270*, 18948−18952.
16. Yang, W., Boggs, K. P., and Jackowski, S. (1995) *J. Biol. Chem. 270*, 23951−23957.

17. Johnson, J. E., Aebersold, R., and Cornell, R. B. (1997) *Biochim. Biophys. Acta 1324*, 273−284.
18. Weber, C. H., Park, Y. S., Sanker, S., Kent, C., and Ludwig, M. L. (1999) *Structure 7*, 1113−1124.
19. Dunne, J. S., Cornell, R. B., Johnson, J. E., Glover, N. R., and Tracey, A. S. (1996) *Biochemistry 35*, 11975−11984.
20. Johnson, J. E., and Cornell, R. B. (1994) *Biochemistry 33*, 4327−4335.
21. Johnson, J. E., Rao, N. M., Hui, S.-W., and Cornell, R. B. (1998) *Biochemistry 37*, 9509−9519.
22. MacDonald, J. I., and Kent, C. (1994) *J. Biol. Chem. 269*, 10529−10537.
23. Friesen, J. A., Campbell, H. A., and Kent, C. (1999) *J. Biol. Chem. 274*, 13384−13389.
24. Bartlett, G. R. (1959) *J. Biol. Chem. 234*, 466−468.
25. Veitch, D. P., and Cornell, R. B. (1996) *Biochemistry 35*, 10743−10750.
26. MacDonald, J. I., and Kent, C. (1993) *Protein Exp. Purif. 4*, 1−7.
27. Cornell, R. B. (1991) *Biochemistry 30*, 5873−5880.
28. Sohal, P. S., and Cornell, R. B. (1990) *J. Biol. Chem. 365*, 11746−11750.
29. Poehling, H.-M., and Neuhoff, V. (1981) *Electrophoresis 2*, 141−147.
30. Veitch, D. P., Gilham, D., and Cornell, R. B. (1998) *Eur. J. Biochem. 255*, 227−234.
31. Sreerama, N., and Woody, R. W. (2000) *Anal. Biochem. 287*, 252−260.
32. Sreerama, N., and Woody, R. W. (1993) *Anal. Biochem. 209*, 32−44.
33. Johnson, W. C., Jr. (1999) *Proteins 35*, 307−312.
34. Greenfield, N. J. (1996) *Anal. Biochem. 235*, 1−10.
35. Sreerama, N., Venyaminov, S. Y., and Woody, R. W. (2001) *Anal. Biochem. 299*, 271−274.
36. Stein, P. E., Leslie, A. G. W., Finch, J. T., and Carrell, R. W. (1991) *J. Mol. Biol. 221*, 941−959.
37. Jones, D. T. (1999) *J. Mol. Biol. 292*, 195−202.
38. Rost, B., and Eyrich, V. A. (2001) *Proteins* Suppl. 5, 192−199.
39. Mao, D., and Wallace, B. A. (1984) *Biochemistry 33*, 2667−2673.
40. Wallace, B. A., and Mao, D. (1984) *Anal. Biochem. 142*, 317−328.
41. Lichtenberg, D. (1985) *Biochim. Biophys. Acta 821*, 470−478.
42. Paternostre, M. T., Roux, M., and Rigaud, J. L. (1988) *Biochemistry 27*, 2668−2677.
43. Saunders, L. (1966) *Biochim. Biophys. Acta 125*, 70−74.
44. Stafford, R. E., Fanni., and Dennis, E. A. (1989) *Biochemistry 28*, 5113−5120.
45. Hennessey, J. P., and Johnson, W. C., Jr. (1981) *Biochemistry 20*, 1085−1094.
46. De Jongh, H. H. J., and de Kruijff, B. (1990) *Biochim. Biophys. Acta 1029*, 105−112.
47. Gow, A., Auton, W., and Smith, R. (1990) *Biochemistry 29*, 1142−1147.
48. Jung, H., Windhaber, R., Palm, D., and Schnackerz, K. D. (1996) *Biochemistry 35*, 6399−6405.
49. Rankin, S. E., Watts, A., and Pinheiro, T. J. T. (1998) *Biochemistry 37*, 12588−12595.
50. Bryson, E. A., Rankin, S. E., Carey, M., Watts, A., and Pinheiro, T. J. T. (1999) *Biochemistry 38*, 9758−9767.
51. Kleinschmidt, J. H., Wiener, M. C., and Tamm, L. K. (1999) *Protein Sci. 8*, 2065−2071.
52. Ladokhin, A. S., and White, S. H. (1999) *J. Mol. Biol. 285*, 1363−1369.
53. Reithmeier, R. A. F., and Deber, C. M. (1992) Intrinsic Membrane Protein Structure: Principles and Prediction in *The Structure of Biological Membranes* (Yeagle, P. L., Ed.) pp 337−393, CRC Press, Boca Raton, FL.
54. Oda, M. N., Forte, T. M., Ryan, R. O., and Voss, J. C. (2003) *Nat. Struct. Biol. 10*, 455−460.
55. Carr, C. M., Chaudhry, C., and Kim, P. S. (1997) *Proc. Natl. Acad. Sci. U.S.A. 94*, 14306−14313.
56. Wang, G., Peterkofsky, A., and Clore, G. M. (2000) *J. Biol. Chem. 275*, 39811−39814.
57. Bernstein, L. S., Grillo, A. A., Loranger, S. S., and Linder, M. E. (2000) *J. Biol. Chem. 275*, 18520−18526.

BI035234K